Appl Petrochem Res (2016) 6:15–23
DOI 10.1007/s13203-015-0115-0

ORIGINAL ARTICLE

Nitrobenzene hydrogenation over Ni/TiO_2 catalyst in vapour phase at atmospheric pressure: influence of preparation method

Mohan Varkolu[1] · Venkateshwarlu Velpula[1] · Ramudu Pochamoni[1] · Ashok Raju Muppala[1] · David Raju Burri[1] · Seetha Rama Rao Kamaraju[1]

Received: 28 January 2015 / Accepted: 4 June 2015 / Published online: 3 July 2015

Abstract Highly dispersed nickel nanoparticles on supports such as ZrO_2 and TiO_2 were prepared by reductive deposition method using hydrazine as reducing agent and applied to nitrobenzene hydrogenation. The highlight of this work is to compare the characteristics and activity of these catalysts with the catalysts of the same composition prepared by impregnation method. All the catalysts were characterized by various techniques such as BET, H_2 pulse chemisorption, TEM, XRD (crystalline nature), reduction behaviour (TPR) and state of nickel species (XPS). Ni/TiO_2 catalyst prepared by reductive deposition method shows excellent conversion of nitrobenzene (99 %) to aniline. This is due to the presence of higher number of surface Ni species than other catalysts as evidenced by H_2-chemisorption. TPR results reveal the formation of metallic Ni species in the reductive deposition method. XRD results suggest that the all catalytic systems show peaks corresponding to the supports only and not due to the metallic Ni because of its presence in highly dispersed form. The decrease in catalytic performance is observed during the time on stream might be due to coking of the catalyst by the reaction intermediate.

Keywords Reductive deposition method · Hydrazine · Ni/TiO_2 · Nitrobenzene · Aniline

✉ Mohan Varkolu
mohan.iict@gmail.com

[1] Inorganic & Physical Chemistry Division, Indian Institute of Chemical Technology, Hyderabad 500007, Telangana, India

Introduction

Nanomaterials are of topical interest, because of their fascinating properties which are different from the corresponding bulk materials. Due to their unique properties, nanomaterials are employed in electronic, optical, catalytic, coating, medical and sensor applications [1–3]. A plethora of research work has been cited on the synthesis of Ni nanoparticles by various methods such as chemical reduction [4], radiolytic reduction [5], UV photolysis [6], solvent extraction reduction [7], microemulsion technique [8], polyol reduction method [9] and sonochemical decomposition [10]. Among these methods, chemical reduction appears to be the most promising method for the large-scale nanoparticle production, although simple methods for preparing metal-supported nanocatalysts under mild and inexpensive conditions have still not been definitely addressed. Among the chemical reduction reagents, utilization of $NaBH_4$ leaves Na^+ ions and B in the catalysts that affect the reaction while the utilization of Na_2HPO_4 leaves both Na^+ ions and P in the catalyst which also influences the catalytic activity. In our present study, we used hydrazine as a reducing agent in the presence of the base at room temperature for 6 h which on decomposition produces H_2 as well as N_2. The liberated N_2 is enough to act as inert atmospheric coverage to the reaction vessel.

Recently, supported nickel catalysts were reported for various organic transformations such as hydrogenation [11–13], steam reforming reactions [14], reductive amination of alcohols [15], hydrodechlorination [16, 17], partial oxidation [18] and dry reforming of methane [19]. Among, hydrogenation is of great interest to both industry and academia.

The synthesis of aniline is generally done by the nitrobenzene (NB) hydrogenation. Aniline is an important

raw material for the synthesis of more than 300 different end products industrially, aniline is mainly used for the production of methylene diphenyl diisocyanate (MDI), a key compound in the production of polyurethane rigid and/or semi-rigid foams and elastomers. It is also used as a solvent, and has been used as an antiknock compound for gasoline [20, 21].

Aniline also finds application in various end-user markets including construction, rubber products, transportation, consumer, adhesives/sealants, packaging, agriculture, textiles, coatings, photography, dyes and pharmaceuticals. A predominant proportion of the worldwide aniline production is utilized in the manufacture of polyurethanes, which are used in a wide array of applications including footwear, insulation and furniture.

The global aniline market is projected to reach 6.2 million tons by the year 2015, due to the increasing demand from various end-user markets. In particular, the rising demand from MDI, the chief ingredient in polyurethane foam, is expected to fuel the consumption of aniline [22].

The present paper highlights the synthesis of Ni catalysts by reductive deposition method compared to impregnation method and as an efficient catalyst for the hydrogenation of NB at atmospheric pressure in the vapour phase.

Experimental

Catalyst preparation

Materials used in this research work are $Ni(NO_3)_2{\cdot}6H_2O$ (M/s. LOBA Chemie, India, 98 %), hydrazine hydrate solution (M/s. LOBA Chemie, India, 80 %), sodium hydroxide (M/s. Sigma Aldrich, USA) and deionized water in the preparation of all the solutions. The nano-sized supported nickel particles were synthesized by dissolving requisite quantities of $Ni(NO_3)_2{\cdot}6H_2O$ in deionized water and placing the respective supports in a vessel. The pH of the solution was then increased to 10 by adding a mixture of sodium hydroxide and hydrazine hydrate solution. The solution is stirred for 6 h. During the stirring, we have observed a change in the colour of the solution from green to violet to colourless and then to grey/black nickel nanoparticles with the evolution of N_2 gas. The liberated N_2 is enough to act as an inert atmospheric blanket. In order to avoid the expansion of volume of N_2 during the stirring, precaution has been taken in selecting a flask of bigger volume. The resultant catalysts were designated as Ni/TiO_2 (R) and Ni/ZrO_2 (R), respectively. In comparison, we have also prepared the catalysts by impregnation method with similar Ni loading. They were designated as Ni/TiO_2 (I) and Ni/ZrO_2 (I), respectively. The Ni loading in all the catalysts was maintained at 5 wt%.

Catalyst characterization

All the above catalysts were characterized by XRD, BET method, H_2 pulse decomposition, TPR and TEM. Details of all the above techniques and procedures have already been described in our previous publication [11–13]. The synthesized catalysts were digested in aqua regia and conducted AAS (M/s. Perkin-Elmer A-300) for Ni content.

Activity studies

Nitrobenzene hydrogenation was carried out in a continuous flow fixed bed reactor operated under atmospheric pressure. In each catalytic run, about 1 g of the catalyst (crushed to 18/25 BSS sieve to eliminate mass transfer limitations) diluted with an equal amount of silica beads to maintain the isothermal conditions, was positioned between two layers of quartz wool at the centre of the reactor comprising 14 mm internal diameter and 300 mm length. The upper portion of the reactor was filled with silica beads that served both as a preheater and a mixer for the reactants. Reaction temperature was continuously monitored by a thermocouple inserted in a thermowell which was placed within the catalyst bed. The liquid reactant was delivered to the reactor from a glass/Teflon air-tight syringe and Teflon tube using a microprocessor-controlled infusion pump (M/s. B. Braun Co, Germany) at a required flow rate. NB and ultra pure H_2 were maintained at a WHSV $\approx$ 1 (h^{-1}) with inlet NB flow = 1 ml h^{-1} and H_2/NB molar ratio = 4.

In a blank test, passage of NB reactant along with a stream of H_2 through an empty reactor or over the support alone did not result in any appreciable NB conversion. The product mixture was cooled in an ice-cooled trap and the analyses were performed on a gas chromatograph (GC-17A, M/s. Shimadzu Instruments Co, Japan) equipped with a programmed split injector and a flame ionization detector, with a OV-1 (30 m length 0.53 mm i.d., 0.33 mm film thickness) capillary column and the product components were confirmed by Shimadzu-17A gas chromatograph equipped along with the mass spectrum QP-8080.

Results and discussion

Hydrazine is normally used as a reducing agent. It can be oxidized depending upon the medium. In acid medium, it easily undergoes oxidation to NH_3 while in case of the basic medium it easily undergoes oxidation to N_2 and H_2. Hence, it is necessary to use the basic medium to produce

N_2 and H_2. For this purpose, we have chosen NaOH as base. The H_2 produced is further utilized for the reduction of nickel precursors which are present in the solution.

In particular, the decomposition of hydrazine takes place in two pathways, which are given as follows:

(i) Complete decomposition (basic medium)
$N_2H_4 \rightarrow N_2\ (g) + 2H_2\ (g)$

(ii) Incomplete decomposition (acid medium)
$3\ N_2H_4 \rightarrow 4NH_3 + 2N_2\ (g)$

X-ray diffraction studies

The XRD patterns of all the catalyst samples are displayed in Fig. 1. In case of Ni/ZrO_2 catalyst, it is reported that peaks at $2\theta = 30.3°$ and 35.14° reveal the presence of indices (111) and (200) planes, respectively corresponding to tetragonal zirconia phase [23]. Major peak at $2\theta = 28.3°$ reveals the part of the sample containing the monoclinic phase of zirconia [24]. It is interesting to note that the incorporation of di-positive or tetra-positive metal ions into the zirconia promotes the transition of tetragonal to monoclinic phase [25, 26]. Furthermore, the pH of the solution during the synthesis was maintained at 10. pH also influences the transformation of zirconia phase [24]. In case of Ni/TiO_2 catalyst, the peaks at $2\theta = 25.32°$, 37.84°, 48.07°, 53.95°, 55.10°, 62.16°, 70.34° and 75.12° reveal the presence of indices (101), (004), (200), (105), (211) (Tetragonal TiO_2, Space group $14_1/amd$ 141)) corresponding to titania (anatase) (ICDD. No. 84-1286). The peaks at around $2\theta = 27.54°$, 37.06° and 43.18° are corresponding to rutile phase of TiO_2. The peaks at around $2\theta = 22.87°$, 34.09° and 49.51° are attributed to $NiTiO_3$ species [27, 28]. Moreover, no peaks corresponding to Ni species were observed and one cannot rule out the formation of Ni species with smaller crystallite sizes (<4 nm), which is the detection limit of XRD technique. From this one can conclude that the Ni species in the catalysts are in highly dispersed state.

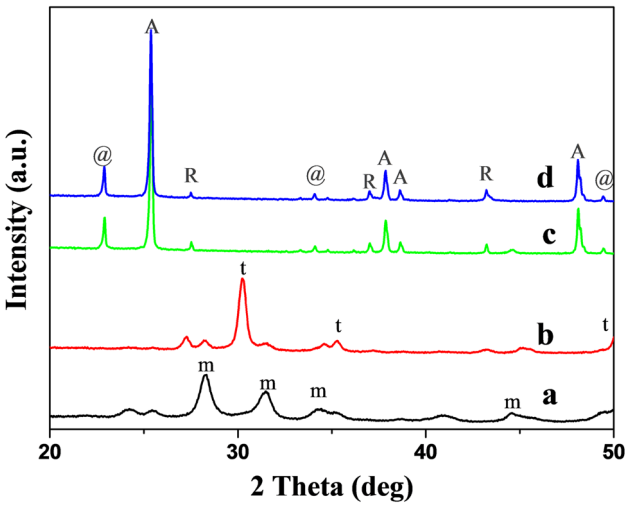

Fig. 1 XRD patterns of Ni catalysts *a* Ni/ZrO_2 (R), *b* Ni/ZrO_2 (I), *c* Ni/TiO_2 (R), *d* Ni/TiO_2 (I). *t* Tetragonal, *m* Monoclinic, *A* Anatase, *R* Rutile and @ $NiTiO_3$

Table 1 Physicochemical properties of Ni catalysts prepared by impregnation and reductive deposition–precipitation method

Catalyst	Ni composition	Surface area (m^2/g)	Pore volume (cm^3/g)	Average pore diameter (Å)
$NiZrO_2$ (R)	4.86	21.08	0.08	155.68
$NiZrO_2$ (I)	5.10	46.90	0.13	109.48
$NiTiO_2$ (R)	4.91	7.97	0.05	234.90
$NiTiO_2$ (I)	4.96	14.60	0.05	147.23

Calculated from atomic absorption spectroscopy

N_2 physisorption studies

The surface area, pore volume and pore size of the catalysts are shown in Table 1. The N_2 adsorption–desorption isotherms of all the catalyst samples are shown in Fig. 2. The surface areas of the catalysts prepared by the reductive deposition precipitation are smaller than that of impregnation method. The surface area of the catalysts prepared by the reductive deposition precipitation is half of the surface area of the catalysts prepared by impregnation method. Although the surface area of the catalysts prepared by reductive deposition method is smaller compared to that of the impregnation method, the catalysts show good yields towards the aniline. The domination of t-ZrO_2 could partially contribute to the higher surface area of the Ni/ZrO_2 catalyst prepared by impregnation method [29, 30]. Although the surface area of Ni/TiO_2 (R) is lower

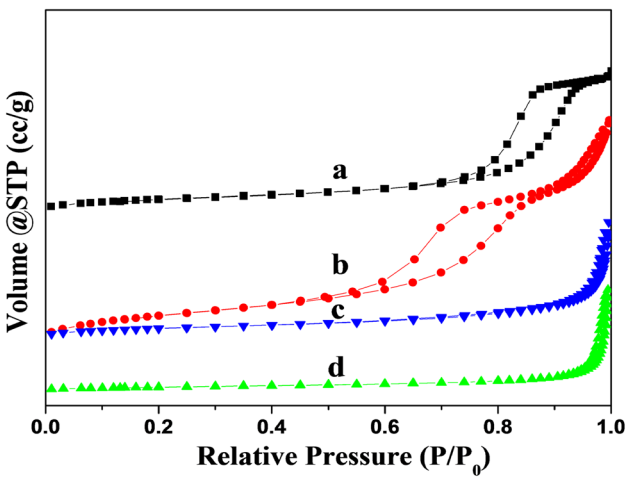

Fig. 2 N_2 adsorption–desorption isotherms of Ni catalysts *a* Ni/ZrO_2(I), *b* Ni/ZrO_2 (R), *c* Ni/TiO_2(I), *d* Ni/TiO_2(R)

Table 2 H_2 uptake, dispersion, metal area and particle size of Ni catalysts

Catalyst	H_2 uptake (μmoles/g)	Dispersion (%)	Average particle size (nm)	TOF (s^{-1})
$NiZrO_2$ (I)	68.66	16.12	6.28	0.0363
$NiZrO_2$ (R)	99.72	23.41	4.31	0.0255
$NiTiO_2$ (I)	119.98	28.17	3.59	0.0135
$NiTiO_2$ (R)	186.82	43.86	2.31	0.0142

compared to Ni/TiO_2 (I), the higher catalytic performance was noticed which could be attributed to the presence of supreme number of surface Ni species (Table 2).

Temperature-programmed reduction studies

Typical profiles of TPR are presented in Fig. 3. For Ni/TiO_2 (I), the reduction peaks at temperatures in the range of 360–480 °C are probably due to the reduction of bulk NiO and NiO with significant interaction with the TiO_2 surface [31]. In the TPR patterns of Ni/ZrO_2 (I), reduction peaks at a T_{max} of about 443 and 503 °C are observed. The former peak can be assigned to the reduction of relatively bulk NiO species and the latter is assumed to be interacted species with ZrO_2 [32]. Presence of strong chemical bonds between the Ni metal and the ZrO_2 has been revealed based on a DFT calculation by Beltran [33]. The reduction peak in the TPR pattern at 306 °C is attributed to the reduction of bulk NiO [33] while the reduction peaks at 420–450 °C were related to NiO_x species that are having strong interaction with ZrO_2 [29, 34]. The strong interaction between the nickel metal and the zirconia could be probably due to an increased interfacial area [29, 34]. While in the case of reductive precipitation catalysts, no significant consumption of hydrogen was observed in their TPR profiles which clearly indicates that the Ni is in its metallic state.

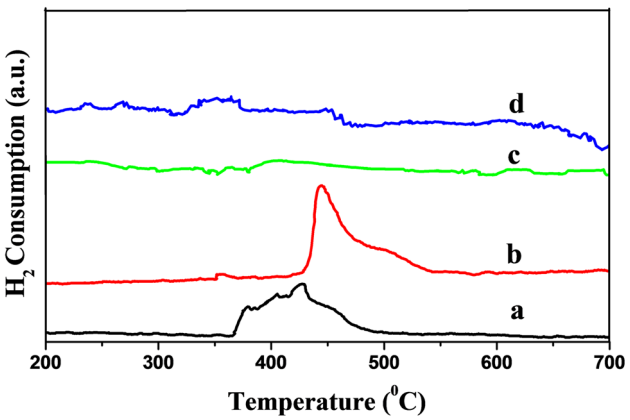

Fig. 3 TPR profiles of Ni catalysts *a* Ni/TiO_2 (I), *b* Ni/ZrO_2 (I), *c* Ni/TiO_2 (R), *d* Ni/ZrO_2 (R)

H_2 pulse chemisorption studies

H_2 chemisorption results are compiled in Table 2. Ni dispersion, and its particle size are determined based on the assumption that each Ni atom chemisorbs one H-atom. The number of surface Ni species on the TiO_2-supported catalysts is more compared to that of the ZrO_2 support and the activity is in good agreement with the H_2 chemisorption results. The metal dispersion follows a trend: Ni/ZrO_2 (I) < Ni/ZrO_2 (R) < Ni/TiO_2 (I) < Ni/TiO_2 (R). This clearly indicates that the metal dispersion depends not only on the preparation method but also on the nature of the support. The smaller particles and higher dispersion are generally useful for the catalytic hydrogenation of NB (Fig. 4).

Microscopic studies

The SEM images of catalysts prepared by reductive deposition–precipitation method show the presence of well-dispersed Ni particles than in the impregnated catalysts. The greater nucleation in the impregnation method leads to agglomeration of metal nanoparticles.

TEM images of Ni/TiO_2 and Ni/ZrO_2 catalysts prepared by impregnation and reductive deposition method are presented in Fig. 5. All the catalysts show highly dispersed amorphous Ni nanoparticles. This is in concurrent with the XRD wherein no peaks corresponding to metallic Ni nanoparticles were noticed. Furthermore, H_2 pulse chemisorption also supports the results such as particle size i.e., below the detection limit of XRD.

XPS studies

The XPS profiles of catalyst samples are displayed in Fig. 6. XPS is a useful technique in order to know the chemical state of Ni. All the reduced samples show two major peaks observed corresponding to the core level of Ni $2P_{3/2}$ and Ni $2P_{1/2}$ transitions at binding energies (BE) of 852.5 and 869.7 eV, which is due to the presence of Nickel in the metallic state. The XPS profile of Ni/TiO_2 (I) seems to be different which might be due to the presence of unreducible NiO species (partial surface oxidation prior to performing the XPS) during the sample transfer.

Catalytic activity studies

Effect of temperature

The catalysts prepared by reductive deposition method are found to be efficient for the production of aniline than for the impregnated catalysts (Fig. 7). Moreover, among all the catalysts Ni/TiO_2 (R) catalyst prepared by reductive

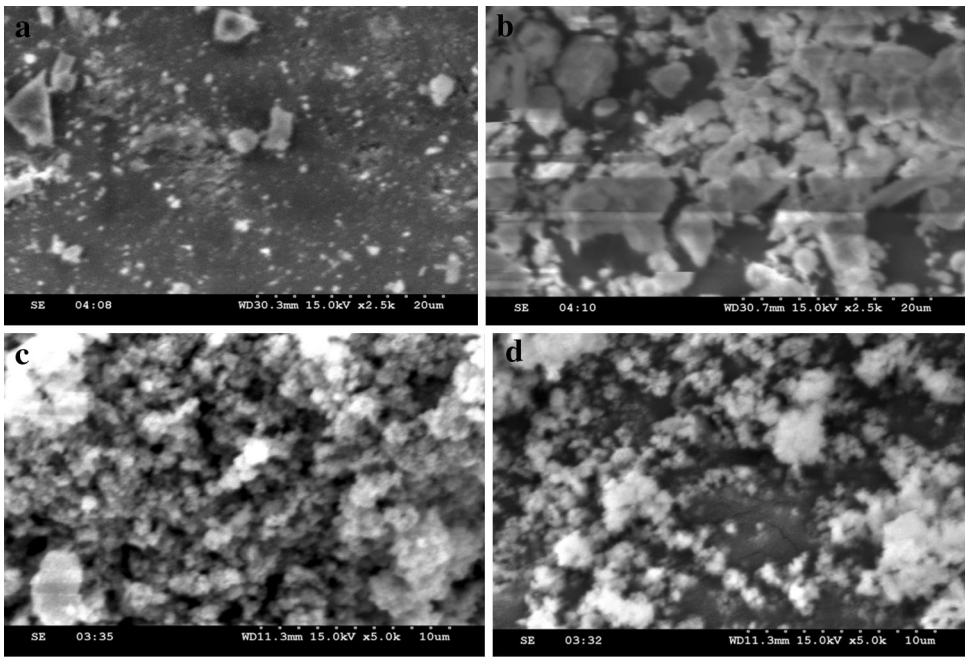

Fig. 4 SEM images of Ni catalysts **a** Ni/TiO_2(R), **b** Ni/TiO_2 (I), **c** Ni/ZrO_2(R), **d** Ni/ZrO_2 (I)

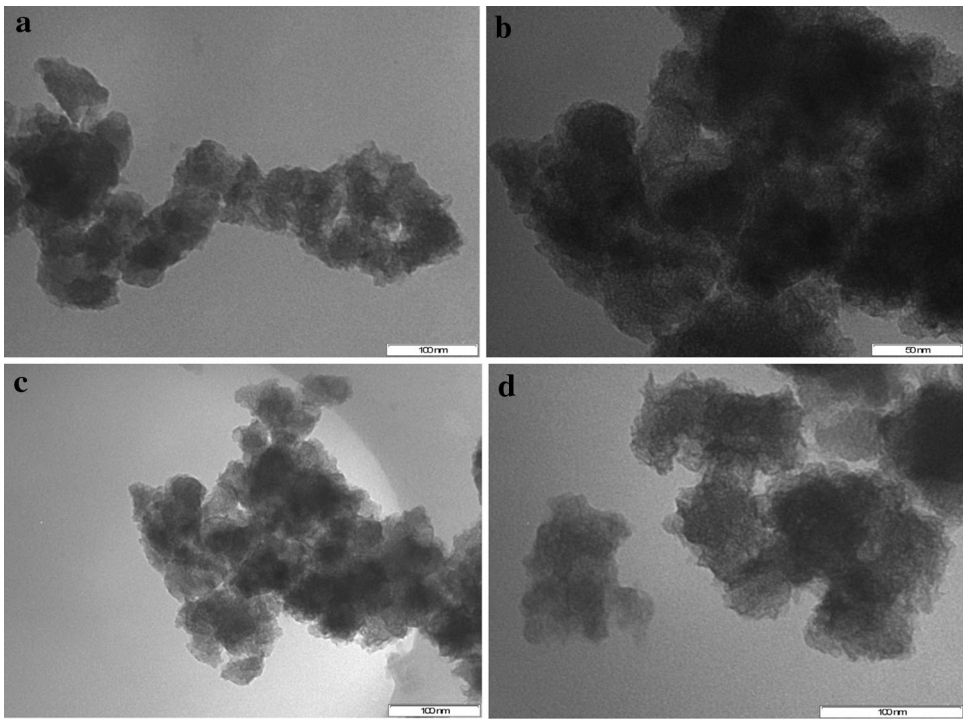

Fig. 5 TEM images of Ni catalysts **a** Ni/TiO_2 (I), **b** Ni/TiO_2 (R), **c** Ni/ZrO_2(I), **d** Ni/ZrO_2 (R)

deposition method is found to be an efficient catalyst due to high dispersion of Ni with smaller Ni particles (Table 2). In addition, the XRD studies, TEM and H_2 pulse chemisorption results also support the presence of smaller Ni particles in this catalyst. Among all the temperatures, 250 °C is found to be an optimum temperature for yielding the aniline at cent percent conversion. Because of the reducible nature of TiO_2, strong metal-support interaction (SMSI) prevails between the Ni and TiO_2. It is noteworthy to mention that the Ni is held strongly by reducible TiO_2 which results in the formation of few $NiTiO_3$ species as evidenced by the XRD pattern (Fig. 1). That's why Ni dispersion and thereby nitrobenzene conversion is higher with this catalyst than in the Ni/ZrO_2 (R). Besides, greater

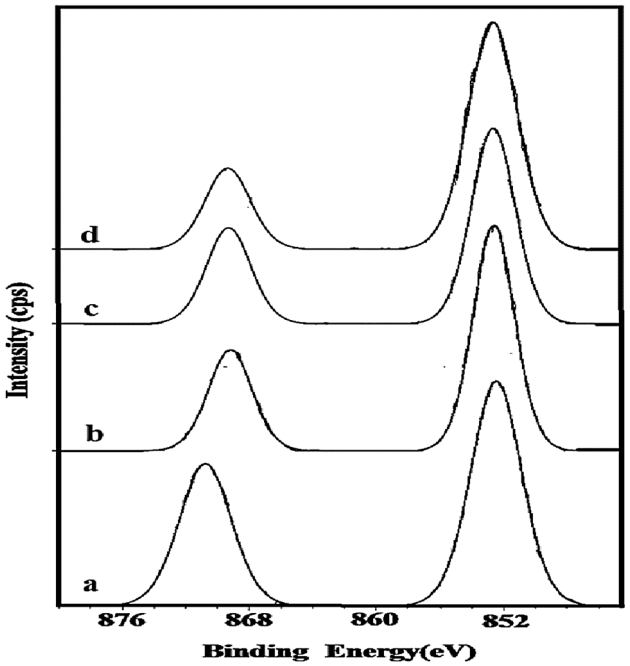

Fig. 6 XPS patterns of reduced Ni catalysts *a* Ni/TiO_2 (I), *b* Ni/ZrO_2 (I), *c* Ni/TiO_2 (R), *d* Ni/ZrO_2 (R)

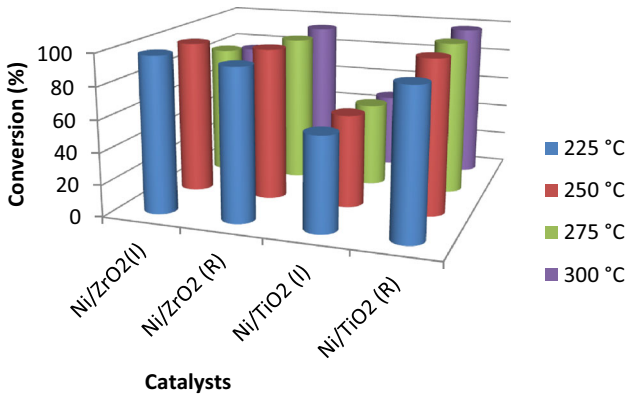

Fig. 7 Effect of support and preparation method on the NB conversion over Ni-based catalysts

number of H_2 uptake was found in the TiO_2-supported Ni catalysts compared to others which might be ascribed to the hydrogen spill-over phenomenon usually found in TiO_2-supported metal catalysts [35].

Effect of time on stream

The stability of Ni/TiO_2 (R) and Ni/ZrO_2 (R) catalysts were prepared by reductive deposition method which can be observed from the Fig. 8, during the time on stream for 10 h at 250 °C. The conversion of NB over Ni/TiO_2 (R) catalyst is decreases slightly during the course of time, which may be due to the condensation of reaction

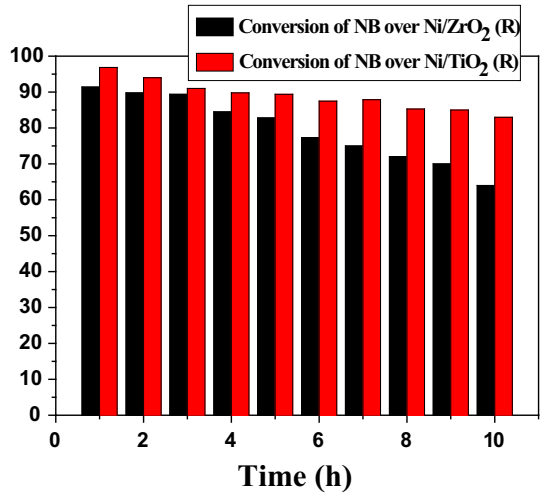

Fig. 8 Time on stream study on Ni/ZrO_2 (R) and Ni/TiO_2 (R) catalysts

intermediates (coke formation) or water released during the reaction. Although the comparable activity of NB was noticed over Ni/ZrO_2 (R) at 250 °C, drastic decrease in activity was observed during time on stream study due to the sintering of Ni particles. The higher sintering of Ni/ZrO_2 (R) could be ascribed to the lower metal-support interaction. While the mild deactivation of Ni/TiO_2 (R) catalyst is owing to higher metal-support interaction. The selectivity towards the aniline is always cent percentage over both the catalysts during the time on stream study. In our previous publication [11], we observed the catalytic performance of Ni/SBA-15 catalyst, during the time on stream for 10 h which remain constant due to hydrophobic nature of SBA-15, while in case of Ni/MgO catalyst, drastic decline in the catalytic performance of NB hydrogenation was observed due to the water adsorption on the MgO support. The adsorbed water may promote brucite–periclase transformation of MgO in case of MgO-supported Ni catalyst. The formation of coke is also another main cause for the deactivation of catalyst during the course of the reaction. Lin et al. [36] studied the NB hydrogenation over Ni/TiO_2 and observed a decline in the activity in subsequent cycles due to the hydrophilic nature of catalyst. In order to avoid the hydrophilic nature, the catalyst was coated with carbon which ultimately decreased the hydrophilic nature of catalyst and found to improve the performance of the catalyst. To know the details of deactivation of the present catalytic systems, we have performed H_2 pulse chemisorption for spent catalysts and the results are presented in Table 3. The results suggest that the decrease in Ni dispersion and increase in average particle size in Ni/ZrO_2(R) spent catalyst is due to sintering of Ni particles which is believed to be responsible for the drastic decrease in catalytic activity. Whereas in the case of

Table 3 H_2 Uptake, dispersion, and particle size of spent Ni catalysts

Catalyst	H_2 Uptake (μmoles/g)	Dispersion (%)	Average particle size (nm)
UNi/ZrO_2 (R)	52.58	12.34	8.19
UNi/TiO_2 (R)	185.95	43.65	2.31

Ni/TiO_2 (R) spent catalysts, we observed an insignificant decrease in Ni dispersion and almost the same Ni particle size when compared to Ni/TiO_2 (R) fresh catalysts which might be caused by high metal-support interactions. Besides, Corma et al., also reported that the deactivation of catalytic system can also happen through the condensation of reaction intermediates [37]. The mild deactivation observed in the case of Ni/TiO_2 (R) catalyst might be due to the condensation of reaction intermediate over the catalyst surface and also its hydrophilic nature.

The turnover frequency (TOF) of NB on each catalyst is defined as the number of moles of NB converted per one surface Ni atom per second [12]. The data are presented in Table 2. Among all the catalysts, the Ni/ZrO_2 (R) catalyst showed greater TOF than the other catalysts. Although the catalyst is showing greater TOF, drastic decrease in conversion was observed during the time on stream presumably due to the agglomeration of Ni nanoparticles (as evidenced from the H_2 chemisorption of the used catalyst). While no such agglomeration was noticed on Ni/TiO_2 (R) catalyst, it could be ascribed to the strong metal-support interaction.

Table 4 highlights the superior performance of the present catalytic system when compared to previously published catalysts for NB hydrogenation in vapour phase conditions. Higher NB conversion (96.5 %) with nearly 100 % selectivity towards aniline at 275 °C was reported over Ru/SBA-15 catalyst at atmospheric pressure when compared to the SiO_2- and Al_2O_3-supported Ru catalysts, which clearly shows the advantage of SBA-15 support [38]. Among the Pd-supported MgO–Al_2O_3 (hydrotalcite) catalysts with different Pd contents, a catalyst with 0.5 wt% Pd exhibited very high NB conversion (97 %) with nearly 100 % selectivity towards AN at atmospheric pressure and at 225 °C [39]. On the other hand, this catalyst suffered activity loss during the time on stream studies, even though, the Pd particle size in the spent catalyst is more or less same as that in the reduced catalyst. The deactivation might, therefore, be due to the water released during the NB hydrogenation. A similar observation was reported over 1 % Pd/MgO–Al_2O_3 catalyst [40]. In our earlier publication, we reported the role of water over Ni/MgO catalyst on the NB hydrogenation activity [11]. It was reported in another publication [41] that higher NB conversion was observed when NB hydrogenation is coupled with 1–4 butanediol dehydrogenation over Cu/MgO catalysts at 250 °C. However, these catalysts also suffered deactivation during time on stream study. It was reported that among the SiO_2-supported Cu catalysts, Cu in combination with Cr and Mo species exhibited good lifetime for the NB hydrogenation reaction [41].

Conclusions

In summary, the catalysts prepared by reductive precipitation method are found to be efficient for the hydrogenation of NB. Among all the catalytic systems, Ni/TiO_2 (R) catalyst shows good conversion of NB as well as selectivity towards aniline which is attributed to the high Ni dispersion having smaller Ni particles along with strong metal-support interaction. However, decrease in conversion during the time on stream analysis is ascribed to the condensation of reaction intermediate on the catalyst surface and also TiO_2 hydrophilic nature. Further efforts will be underway to get efficient catalytic system for consistent catalytic performance for longer lifetime to meet the current demand for aniline.

Table 4 Comparison of nitrobenzene hydrogenation activities of 5 wt% Ni/TiO_2 (R) catalyst with the reported catalysts

Catalyst	Operating conditions		NB conversion (%)	AN selectivity (%)	Reference
	Temperature (°C)	H_2/NB			
4.5 wt% Ru/SBA-15	275	4	94	100	[38]
0.5 wt% Pd/HT	225	4	97	100	[39, 40]
5 wt% Ni/SBA-15	250	4	99	100	[11]
25 wt% Cu/MgO	280	4	94	100	[41]
Cu/SiO_2	260	4	99	100	[42–44]
10 wt% Cu/HT (impregnation method)	225	3	72	100	
10 wt% Cu/HT (Co-precipitation method)	275	3	68	100	
5 wt% Ni/TiO_2 (R)	250	4	99	100	Present case

Acknowledgments The authors are grateful to the Council of Scientific and Industrial Research, New Delhi, India for the facilities and financial support.

References

1. Frank S, Lauterbur PC (1993) Voltage-sensitive magnetic gels as magnetic resonance monitoring agents. Nature 334:363
2. Yamaguchi K, Matsumoto K, Fujii T (1990) Magnetic anisotropy by ferromagnetic particles alignment in a magnetic field. J Appl Phys 67:4493
3. Prinz GA (1998) Magnetoelectronics. Science 282:1660
4. Choi JY, Lee KY, Kim BK, Kim JM (2005) A chemical route to large-scale preparation of spherical and monodisperse Ni powders. J Am Ceram Soc 88:3020
5. Hodak JH, Henglein A, Giersig M, Hartland GV (2000) Laser-induced inter-diffusion in AuAg core-shell nanoparticles. J Phys Chem B 104:11708
6. Remita S, Mostafavi M, Delcourt MO (1996) Bimetallic Ag-Pt and Au-Pt aggregates synthesized by radiolysis. Radiat Phys Chem 47:275
7. Brust M, Walker M, Bethell D, Schiffrin DJ, Whyman R (1994) Synthesis of thiol-derivatised gold nanoparticles in a two-phase liquid–liquid system. J Chem Soc Chem Commun 7:801
8. Chen DH, Wu SH (2000) Synthesis of nickel nanoparticles in water-in-oil microemulsions. Chem Mater 12:1354
9. Dutta D, Borah BJ, Saikia L, Pathak MG, Sengupta P, Dutta DK (2011) Synthesis and catalytic activity of Ni-acid activated montmorillonite nanoparticles. Appl Clay Sci 53:650
10. Mizukoshi Y, Okitsu K, Maeda Y, Yamamoto TA, Oshima R, Nagata Y (1997) Sonochemical preparation of bimetallic nanoparticles of gold/palladium in aqueous solution. J Phys Chem B 101:7033
11. Mohan V, Pramod CV, Suresh M, Reddy KHP, Raju BD, Rao KSR (2012) Advantage of Ni/SBA-15 catalyst over Ni/MgO catalyst in terms of catalyst stability due to release of water during nitrobenzene hydrogenation to aniline. Catal Commun 18:89
12. Mohan V, Raghavendra C, Pramod CV, Raju BD, Rao KSR (2014) Ni/H-ZSM-5 as a promising catalyst for vapour phase hydrogenation of levulinic acid at atmospheric pressure. RSC Adv 4:9660
13. Mohan V, Venkatehwarlu V, Pramod CV, Raju BD, Rao KSR (2014) Vapour phase hydrocyclisation of levulinic acid to γ-valerolactone over supported Ni catalysts. Catal Sci Technol 4:1253
14. Borowieek T, Golebiowski A, Stasinska B (1997) Effects of small MoO_3 additions on the properties of nickel catalysts for the steam reforming of hydrocarbons. Appl Catal A 153:141
15. Dume C, Holderich WF (1999) Amination of 1-octanol. Appl Catal A 183:167
16. Chary KVR, Rao Ramana PV, Vishwanthan V (2006) Synthesis and high performance of ceria supported nickel catalysts for hydrodechlorination reaction. Catal Commun 7:974
17. Cesteros Y, Salagre P, Medina F, Sueiras JE (1999) Appl Catal B 22:135
18. Miao Q, Xiong GX, Sheng SS, Cui W, Xu L, Guo XX (1997) Partial oxidation of methane to syngas over nickel-based catalysts modified by alkali metal oxide and rare earth metal oxide. Appl Catal A 154:17
19. Kim JH, Suh DJ, Park TJ, Kim KL (2000) Effect of metal particle size on coking during CO_2 reforming of CH_4 over Ni–alumina aerogel catalysts. Appl Catal A 197:191
20. U.S. Environmental Protection Agency (1985) Health and Environmental Effects Profile for Aniline. Environmental Criteria and Assessment Office, Office of Health and Environmental Assessment, Office of Research and Development, Cincinnati
21. Budavari S (1989) The Merck index. An encyclopedia of chemicals, drugs, and biologicals, 11th edn. Merck and Co. Inc., Rahway
22. http://www.prweb.com/releases/aniline/amino_benzene/prweb4370264.htm. Accessed 11 Aug 2010
23. Das SK, Bhunia MK, Sinha AK, Bhaumik A (2009) Self-assembled mesoporous zirconia and sulfated zirconia nanoparticles synthesized by triblock copolymer as template. J Phys Chem C 113:8918
24. Peters A, Nouroozi F, Richter D, Lutecki M, Gläser R (2011) Nickel-loaded zirconia catalysts with large specific surface area for high-temperature catalytic applications. ChemCatChem 3:598
25. Gawande MB, Jayaram RV (2006) A novel catalyst for the Knoevenagel condensation of aldehydes with malononitrile and ethyl cyanoacetate under solvent free conditions. Catal Commun 7:931
26. Monte FD, Larsen W, Mackenzie JD (2000) Chemical interactions promoting the ZrO_2 tetragonal stabilization in ZrO_2–SiO_2 binary oxides. J Am Ceram Soc 83(6):1506
27. Chuang SH, Hsieh ML, Wu SC, Lin HC, Chao TS, Hou TH (2011) Fabrication and characterization of high-k dielectric nickel titanate thin films using a modified sol-gel method. J Am Ceram Soc 94(1):250
28. Joseph Antony Raj K, Prakash MG, Mahalakshmy R, Elangovan T, Viswanathan B (2012) Selective hydrogenation of acetophenone over nickel supported on titania. Catal Sci Technol 2:1429
29. Li S, Zhang C, Huang Z, Wu G, Gong J (2013) A Ni@ ZrO_2 nanocomposite for ethanol steam reforming: enhanced stability via strong metal–oxide interaction. Chem Commun 49:4226
30. Yamaguchi T (1994) Application of ZrO_2 as a catalyst and a catalyst support. Catal Today 20:199
31. Ho SW, Chu CY, Chen SG (1998) Effect of thermal treatment on the nickel state and CO hydrogenation activity of titania-supported nickel catalysts. J Catal 178:34
32. Roh HS, Koo KY, Jeong JH, Seo YT, Seo DJ, Seo YS, Yoon WL, Park SB (2007) Combined reforming of methane over supported Ni catalysts. Catal Lett 117(1–2):85
33. Tomiyama S, Takahashi R, Sato S, Sodesawa T, Yoshida S (2003) Preparation of Ni/SiO_2 catalyst with high thermal stability for CO_2-reforming of CH_4. Appl Catal A 241:349
34. Beltran JI, Gallego S, Cerda J, Moya JS, Munoz MC (2003) Bond formation at the Ni/Z rO_2 interface. Phys Rev B 68:075401
35. Inui T, Fujimoto K, Uchijima T, Masai M (eds) (1993) New aspects of spillover effect in catalyst. In: Stud. Surf. Sci. Catal., vol 77, Elsevier, Amsterdam
36. Lin W, Cheng H, Ming J, Yu Y, Zhao F (2012) Deactivation of Ni/TiO_2 catalyst in the hydrogenation of nitrobenzene in water and improvement in its stability by coating a layer of hydrophobic carbon. J Catal 291:149
37. Corma A, Concepcion P, Serna P (2007) A different reaction pathway for the reduction of aromatic nitro compounds on gold catalysts. Angew Chem Ind Ed 46:7266

38. Chary KVR, Srikanth CS (2009) Selective hydrogenation of nitrobenzene to aniline over Ru/SBA15 catalysts. Catal Lett 128:164
39. Sangeetha P, Seetharamulu P, Shanthi K, Narayanan S, Rama Rao KS (2007) Studies on Mg-Al oxide hydrotalcite supported Pd catalysts for vapor phase hydrogenation of nitrobenzene. J Mol Catal A Chem 273:244
40. Sangeetha P, Shanthi K, Rama Rao KS, Viswanathan B, Selvam P (2009) Hydrogenation of nitrobenzene over palladium-supported catalysts—effect of support. Appl Catal A 353:160
41. Hari Prasad Reddy K, Rahul R, Sree Vardhan Reddy S, David Raju B, Rama Rao KS (2009) Coupling of 1,4-butanediol dehydrogenation reaction with the hydrogenation of nitrobenzene over Cu/MgO catalysts. Catal Commun 10:879
42. Fang X, Yao S, Qing Z, Li F (1997) Study on silica supported Cu-Cr-Mo nitrobenzene hydrogenation catalysts. Appl Catal A 161:129
43. Pramod CV, Suresh M, Mohan V, Sridevi B, David Raju B, Rama Rao KS (2012) Coupling of cyclohexanol dehydrogenation-nitrobenzene hydrogenation over MgO-Al_2O_3 hydrotalcite supported Cu catalysts: effect of Cu loading. Curr Catal 1:140
44. Pramod CV, Mohan V, David Raju B, Rama Rao KS (2013) An efficient use of hydrogen for the simultaneous synthesis of cyclohexanone and aniline over Cu–MgO–Al_2O_3 (hydrotalcite like precursor) catalyst. Catal Lett 143:432